analytical chemistry

ARTICLE

pubs.acs.org/ac

Microfabricated Renewable Beads-Trapping/Releasing Flow Cell for Rapid Antigen−Antibody Reaction in Chemiluminescent Immunoassay

Zhifeng Fu,[†,‡] Guocheng Shao,[‡,§] Jun Wang,[*,‡] Donglai Lu,[‡] Wanjun Wang,[§] and Yuehe Lin[*,‡]

[†]Key Laboratory of Luminescence and Real-Time Analysis (Ministry of Education), College of Pharmaceutical Sciences, Southwest University, Chongqing 400716 China

[‡]Pacific Northwest National Laboratory, Richland, Washington 99352, United States

[§]Department of Mechanical Engineering, Louisiana State University, Baton Rouge, Louisiana 70803, United States

Supporting Information

ABSTRACT: A renewable flow cell integrating a microstructured pillar-array filter and a pneumatic microvalve was microfabricated to trap and release beads. A bead-based immunoassay using this device was also developed. This microfabricated device consists of a microfluidic channel connecting to a beads chamber in which the pillar-array filter is built. Underneath the filter, there is a pneumatic microvalve built across the chamber. Such a device can trap and release beads in the chamber by "closing" or "opening" the microvalve. On the basis of the pneumatic microvalve, the device can trap beads in the chamber before performing an assay and release the used beads after the assay. Therefore, this microfabricated device is suitable for "renewable surface analysis". A model analyte, 3,5,6-trichloropyridinol (TCP), was chosen to demonstrate the analytical performance of the device. The entire fluidic assay process, including beads trapping, immuno binding, beads washing, beads releasing, and chemiluminesence signal collection, could be completed in 10 min. The immunoassay of TCP using this microfabricated device showed a linear range of 0.20−70 ng/mL with a limit of detection of 0.080 ng/mL. The device was successfully used to detect TCP spiked in human plasma at the concentration range of 1.0−50 ng/mL, with an analytical recovery of 81−110%. The results demonstrated that this device can provide a rapid, sensitive, reusable, low-cost, and automatic tool for detecting various biomarkers in biological fluids.

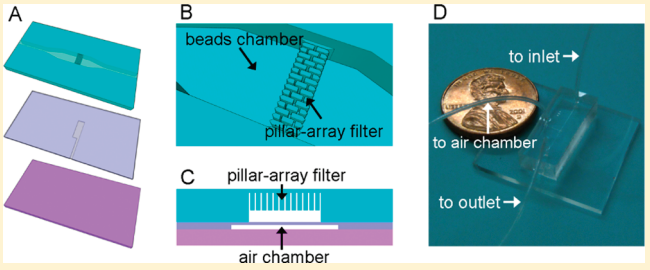

The significance of immunoassays has been demonstrated in many vital fields, including clinical diagnosis, environmental monitoring, homeland security, and food analysis.[1,2] An automatic rapid immunoassay can be achieved by combining a programmed flow injection (FI)/sequential injection (SI) system with antibody-immobilized microarray,[3] capillary,[4,5] bead,[6−10] and polymer membrane.[11,12] Miniaturizing these FI/SI immunoassays offers some advantages over the conventional larger scale robotic fluidic systems, although there are still some problems to be solved. The smaller dimensions of a microfabricated device can greatly reduce the consumption of expensive immunoreagents and precious samples as well as wastes. Also, the reduction in liquid volumes required for sampling, fluid transfer, and immunoreactor flushing translates into a shorter run time, lower power requirements, and better portability.[2,13−15]

For heterogeneous immunoassays in a microfabricated device, antibodies are immobilized on either surface of a microchannel[13,16−24] or micrometer-dimension beads captured in a device.[25−31] For the former method, although the diffusion distance in the microchannel is greatly reduced in comparison to the conventional microtiter plate-based approaches, the mass transport of the analyte is still limited in the microchannel at a very low concentration. This is because of the slow planar diffusion on the flat surface, which is disadvantageous to reduce the incubation time and improve the assay speed.[2] Also, the limited amount of immobilized antibodies/antigens resulting from the small surface area of a microchannel leads to a negative effect on the assay sensitivity. Furthermore, most of the reported channel surface-based microfabricated devices are disposable and suffer from high consumables cost since the fabrication of a miniaturized device is always time consuming and labor intensive. For the latter method, a bead with a small size offers a high surface-to-volume ratio for immobilizing a large amount of antibodies/antigens, which can greatly improve the sensitivity of immunoassays. Moreover, a reduced transport distance for immunoreagents can accelerate the binding when immunoreagents flow

Received: December 7, 2010
Accepted: February 12, 2011
Published: March 02, 2011

through packed beads because of the increase of mass transport in the continuous flow of the fluid in the device. A magnetic bead shows great promise for developing reusable microfabricated immunoassay devices because using a magnetic bead as the immunoreactor in a microfluidic platform enables the convenient trapping and releasing of beads by manipulating the external magnet.[25−27] For nonmagnetic (polystyrene, glass, resin, etc.) bead-based fluidic systems, mechanical trapping microstructures are often fabricated to hold beads and pass fluids. A microweir[26−29] and a filter array[32] consisting of gaps are two common microstructures for this purpose in which the beads with a size larger than the gaps can be held by the weir or the filter while all the fluids are free to pass through the packed beads and the trapping microstructure. Although these designs using nonmagnetic beads are much simpler and more versatile for various bead-based microfluidic immunoassays, unfortunately, no beads-releasing function was considered for the purpose of multiple uses. Therefore, unlike the conventional larger scale "beads injection" systems[6,9,10] and the microfabricated magnetic bead-manipulating device,[25−27] most of those nonmagnetic bead-based microfabricated devices have to be discarded after only one use. Thus, because of the high cost of fabrication, the assays may be much more expensive considering that the device can only be used once.

The popularity of "photolithography" has led to the development of pressure-controlled pneumatic microvalves suitable for integration into an all-elastomer microfabricated device. By adjusting the gas pressure, a pneumatic microvalve can be conveniently actuated to precisely control fluids in a microfabricated device.[33,34] Microfabricated devices integrated with a pneumatic microvalve have already been reported in the fields of genetic analysis,[35] amino acid detection,[36] protein structure studies,[37] etc., indicating their great potential in fluid control for developing microfabricated analysis systems. To date, there has been no report on the use of pneumatic microvalves to manipulate solid beads in the microchannel for immunoassays.

We designed a microfabricated renewable beads-trapping/releasing flow cell for a fluidic bioassay. Using polydimethylsiloxane (PDMS)-based photolithography technology, a device integrating a microstructured pillar-array filter and a pneumatic microvalve was fabricated for FI/SI analysis. By "opening" and "closing" the microvalve, beads can be conventionally manipulated in the device to perform a fluidic bead-based immunoassay. A metabolite of chlorpyrifos, 3,5,6-trichloropyridinol (TCP), was used as a model analyte to test this device for a rapid chemiluminescent (CL) immunoassay. Since TCP is a biomarker of exposure to chlorpyrifos, one of the most widely used organophosphorus pesticides across the world, it is important to develop a rapid, sensitive, and low-cost method for TCP detection.[38−40] The results show that the assay performed on this device is simple, rapid, and sensitive for TCP. Therefore, this device may open a new avenue for detecting other biomarkers, such as proteins.

EXPERIMENTAL DETAILS

Reagents and Materials. A mouse monoclonal TCP antibody solution at 2.0 mg/mL was provided by Strategic Diagnostics, Inc. (Newark, DE). TCP, phosphate buffer saline at pH 7.4 (PBS, 0.010 M), bovine serum albumin (BSA), *N*-hydroxysuccinimide (NHS), hexamethyldisilazane, *N*,*N*′-dimethylformamide (DMF), and Tween-20 were all purchased from Sigma-Aldrich (St. Louis, MO). Human heparin plasma was purchased from Golden West Biologicals, Inc. (Temecula, CA). A suspension of carboxyl-functionalized polystyrene beads (9.8 μm diameter, 9.7% solids content) and a PolyLink protein coupling kit were obtained from Bangs Laboratories, Inc. (Fishers, IN). The PolyLink protein coupling kit was composed of 1-ethyl-3-(3-dimethylaminopropyl)carbodiimide (EDC), a coupling buffer, and a wash/storage buffer. A SuperBlock blocking buffer was provided by Thermo Fisher Scientific, Inc. (Rockford, IL). A horseradish peroxidase (HRP) CL substrate reagent kit consisting of Reagent A (luminol) and Reagent B (enhancer) was obtained from Invitrogen Corp. (Carlsbad, CA). A PDMS elastomer kit (Sylgard 184) was purchased from Dow Corning Corp. (Midland, MI). A negative-ton photoresist SU-8 25, SU-8 50, and SU-8 developer were provided by Microchem Corp. (Newton, MA). Silicon wafers with a 10-cm diameter were purchased from Universitywafer, Inc. (South Boston, MA). HRP−TCP conjugate was home synthesized with an EDC-NHS strategy (see Supporting Information). A disposable PD-10 desalting column packed with Sephadex G-25 medium was provided by GE Healthcare Biosciences (Pittsburgh, PA). A centrifugal filter device (Amicon Ultra, MWCO 3.5 K) was purchased from Millipore Corp. (Billerica, MA). Ultrapure water (18.2 MΩ) purified with the Nanopure System (Barnstead, Kirkland, WA) was used in the entire investigation.

Preparation of Antibody-Coupled Beads. First, a 125-μL suspension of carboxyl-functionalized polystyrene beads was washed twice with the coupling buffer and centrifuged for 2 min at 10 000 rmp to remove the supernatant waste. The beads were then redispersed in 0.50 mL of coupling buffer, in which 10 mg of EDC and 5.0 mg of NHS were added to activate the carboxyl groups for 30 min under constant stirring at room temperature (RT). The activated beads were washed twice with PBS with the aid of centrifugation and redispersed in 100 μL of PBS. Fifty microliters of TCP antibody at 2.0 mg/mL was then dissolved in the suspension and reacted with the activated beads under gentle stirring at RT for 2.5 h. The resulting antibody-coupled beads were washed using the wash/storage buffer five times and separated by a centrifuge with the same protocol as described above. Then the beads were redispersed in 475 μL of this buffer at 4 °C until used.

Fabrication and Characterization of the Renewable Device. The PDMS-based microfabricated device, as shown in Figure 1A−D, was composed of a beads chamber layer, a pneumatic control layer, and a glass substrate. A photolithography technique was employed for fabricating the PDMS layers of the device. The Supporting Information describes the preparation of the molds for the beads chamber layer and the pneumatic control layer. The base and curing agents of the elastomer kit were mixed at a ratio of 10:1 to prepare the PDMS precursor. Vacuum was applied to remove the bubbles from the PDMS precursor prior to use. To prepare the beads chamber layer, the PDMS precursor was directly poured onto the mold to obtain a 3-mm-thick PDMS layer. For the pneumatic control layer, the PDMS precursor was spin coated on the mold at a rotation rate of 2000 rpm for 30 s to obtain a membrane with a thickness of 50 μm. Both layers were thermally cured at 75 °C for 2 h. The beads chamber layer was then peeled from the mold and punched to obtain an outlet and an inlet with an inner diameter of 0.70 mm. Both layers were then treated in an oxygen plasma (PX-250 March Plasma Systems, March Instruments Inc., Concord, CA) for 30 s. Immediately after the plasma treatment, the beads chamber layer was aligned onto the air chamber layer and cured at 75 °C for another 20 min. The resulting double-layer PDMS

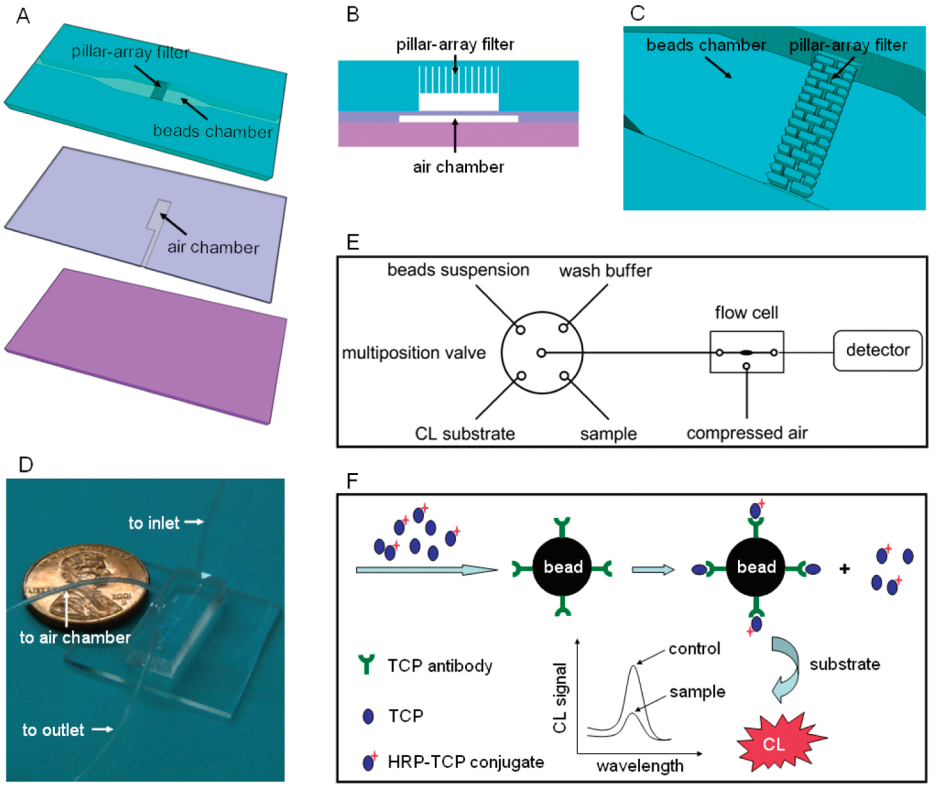

Figure 1. Schematic illustration of the microfabricated renewable flow cell for trapping/releasing beads and the competitive immunoassay of TCP. (A) Perspective diagrams for the three layers of the flow cell: the beads chamber layer, the pneumatic control layer, and the glass substrate (from top to bottom). (B) Cross-section view of the flow cell. (C) Enlarged view of the beads chamber. (D) Photograph of the flow cell. (E) Fluidic immunoassay system for TCP detection. (F) Detection scheme of competitive immunoassay of TCP on beads.

assembly was peeled from the mold. After pneumatic access hole punching, the double-layer assembly and the glass substrate were treated in an oxygen plasma for 30 s, assembled together, and cured at 75 °C for 2 h to form an irreversible bond. Finally, three tygon tubes (i.d. 0.25 mm, o.d. 0.76 mm, Cole-Parmer, Inc., Vernon Hills, IL) were plugged into the pneumatic access hole, the fluid inlet, and the fluid outlet of the elastomer device to form a microfabricated flow cell illustrated in Figure 1A–D. A Super-Block blocking buffer was applied to block the nonspecific binding sites in the channel and the beads chamber of the PDMS device (10 min).

The micrographs (Figure 2) of the microfabricated PDMS flow cell were obtained using a VHX-600 Digital Microscope (Keyence Corp., Osaka, Japan).

Assembly of Fluidic Assay System. The fluidic immunoassay system using the beads-trapping/releasing flow cell was constructed as shown in Figure 1E, in which all components were connected with tygon tubes. All fluids were driven with the syringe pumps (BASi Corp., West Lafayette, IN). Different fluids were sequentially introduced into the microfabricated PDMS device with a multiposition valve with multiple inlets and one common outlet (Global FIA, Inc., Fox Island, WA). The CL signals were collected by a Safire^2 Multimode Reader (Tecan Group Ltd., Männedorf, Switzerland).

Fluidic Assay Protocol. A CL immunoassay of TCP was performed in a competitive mode illustrated in Figure 1F. First, 40 psi air pressure was applied to the air chamber so that the flow cell was set to the "trapping" mode. To prevent the compressed air from penetrating through the ventilated PDMS membrane and forming bubbles in the beads chamber, the air chamber was filled with water before the air pressure was applied. Then 15 μL of a diluted suspension of antibody-coupled beads (50-fold diluted in 2% BSA) was injected into the beads chamber at a flow rate of 100 μL/min. The quantity of the beads in the suspension was estimated to be about 18 800. Once the beads were trapped by the filter, 15 μL of 1:1 mixed sample and HRP–TCP conjugate (2.0 μg/mL in 2% BSA) was perfused through the trapped beads at a flow rate of 2.0 μL/min. Then the trapped beads were washed by PBS containing 0.05% Tween-20 at a flow rate of 50 μL/min for 1 min to remove unbound TCP and HRP–TCP conjugate. To collect beads for signal detection, the air pressure applied to the air chamber was withdrawn so that the flow cell was set to the "releasing" mode, and then 50 μL of CL substrate solution (1:1 freshly mixed Reagent A and Reagent B) was injected into the beads chamber to flush out all the beads at a flow rate of 100 μL/min. The CL signal from the expelled suspension was detected to quantify TCP in the samples. After washing using 50 μL of wash buffer at a flow rate of 100 μL/min, the assay system was ready for the next assay. The whole assay time, including beads trapping, immuno binding, washing, beads releasing, and signal detection, was about 10 min.

RESULTS AND DISCUSSION

Device Design and Working Principle. The design of a microfabricated reusable flow cell for bead-based immunoassays needs to meet the following two requirements: (1) the flow resistance must remain low enough to ensure free passage of the fluid at all phases, even at the "valve closing" mode, and (2) the trapped beads can be easily released so that the device can be

dx.doi.org/10.1021/ac1032116 |Anal. Chem. 2011, 83, 2685–2690

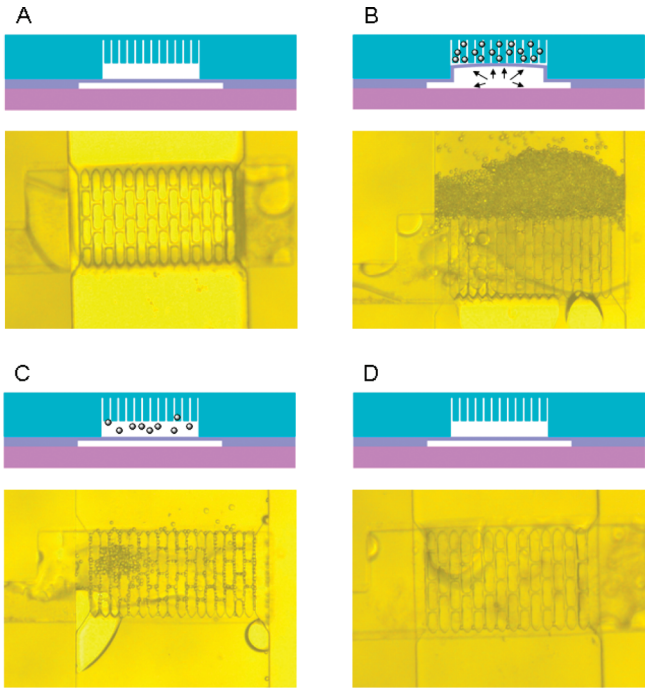

Figure 2. Principle of the flow cell illustrated in side view cross-section (upper) and micrographs of beads chamber in top view (lower) at the stages of (A) before trapping, (B) trapping, (C) releasing, and (D) after releasing.

used repeatedly. As illustrated in Figures 1A−C and 2, the pillar array of the filter in the beads chamber has a "brick wall"-like pattern across the whole chamber width. The dimensions of each pillar are 20 μm × 50 μm, and the interval distance between the adjacent pillars is 5 μm, which enables the free passage of fluids through the filter, while the beads with a size of more than 5 μm in diameter can be held. The pillars at the front and the end of the "brick wall" are designed as triangles for low flow resistance and good flow homogeneity across the whole chamber. The width of the flow channel and the beads chamber is 200 and 500 μm, respectively. The depth of the pillar array and the beads chamber is 45 and 75 μm, respectively; thus, a 30-μm gap is formed between the pillar-array filter and the bottom of the beads chamber. An air chamber integrated in the pneumatic control layer is located under the beads chamber, and its size matches that of the "brick wall". The membrane between the beads chamber and the air chamber is 20-μm thick.

The principle of this beads-trapping/releasing device is illustrated in Figure 2. If no pressure was applied to the air chamber, the upper membrane of the pneumatic microvalve was relaxed (Figure 2A), which enabled the 9.8-μm beads to freely pass through the 30-μm gap between the pillar-array filter and the beads chamber bottom. This state was defined as "valve opening". Once adequate pressure was applied to the air chamber, the upper membrane deformed until it reached the bottom of the filter. At this "valve closing" state, all beads were retained in the beads chamber because the beads were larger than the intervals between the adjacent pillars (Figure 2B). However, all liquid reagents, including sample solution and wash buffer, were still able to freely flow through the packed beads and the pillar-array filter to perform immuno binding and beads washing. After beads washing, pressure in the air chamber was withdrawn to "open" the pneumatic valve. At this stage, beads were freely passed through the gap along with the fluid (Figure 2C). It was also seen

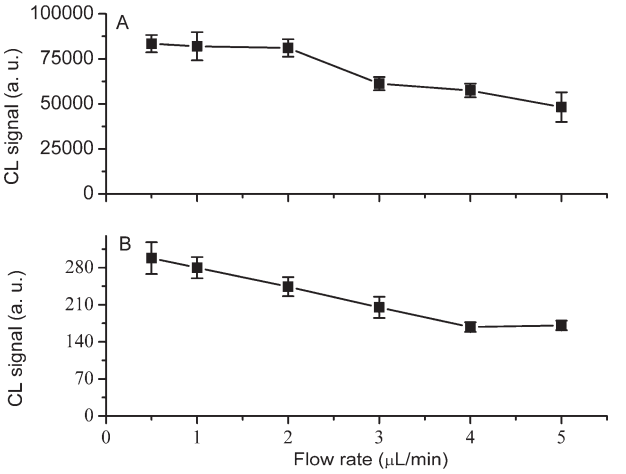

Figure 3. CL signals resulting from (A) immuno binding and (B) nonspecific binding at different flow rates for 15 μL of HRP−TCP conjugate at 1.0 μg/mL, where n = 5 for each point.

in Figure 2D that almost all beads had been successfully expelled out of the flow cell after 30 s of perfusion. Therefore, by "closing" and "opening" the microvalve, beads trapping and releasing were conveniently realized to perform "surface renewable analysis".

The principle of the competitive immunoassay of TCP in this device is shown in Figure 1 F. TCP in the sample resulted in less HRP−TCP conjugate binding to the beads and lower CL signal. Therefore, this can be used for quantitation of TCP in the samples.

Experimental Conditions Optimization for TCP Competitive Immunoassay. The immuno-binding time, which is usually controlled by mass transport of immunoreagents, is a bottleneck preventing the improvement of the speed of a conventional immunoassay. In this fluidic bead-based competitive immunoassay, the reagent liquid flow in the beads chamber constantly renewed the TCP and HRP−TCP conjugate at the surface of the antibody-coupled beads, which led to faster immuno binding. In contrast, an immunoassay in the conventional static mode solely depends on the molecules diffusing to bring about the interactions. In addition, the diffusion distance between interacting molecules in a microwell is in the magnitude of millimeter compared to micrometer in the beads chamber. These factors resulted in faster binding and therefore reduced immunoreaction time in this microfabricated device and ultimately led to a much shorter run time compared to conventional static techniques. To study the influence of the antigen flow rate to the immuno-binding efficiency at RT, 15 μL of 1.0 μg/mL HRP−TCP conjugate (in 1% BSA) was passed through the beads chamber at different flow rates. A control experiment was also performed to study nonspecific binding at different flow rates by using BSA-coupled beads instead of TCP antibody-coupled beads. As seen in Figure 3A, immuno binding reached a maximum when the flow rate of the HRP−TCP conjugate decreased to 2.0 μL/min, which meant the binding process could be completed in 7.5 min. Also, it was found that the signal from nonspecific binding at this flow rate was negligible (Figure 3B). Therefore, this flow rate was employed for immuno binding. As a comparison, the same amounts of HRP−TCP conjugate and beads were incubated in a centrifuge tube at 37 °C. Due to the small volume of the suspension (30 μL in total) and the high density of the beads, the beads always tended to precipitate, even though the suspension

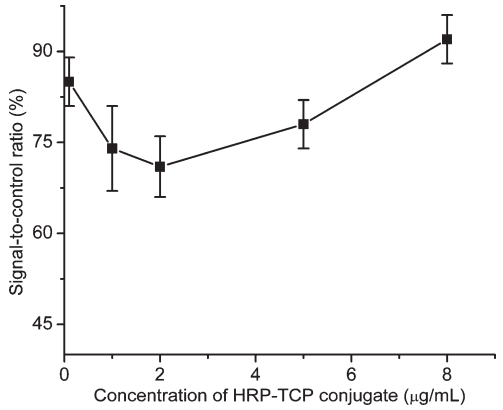

Figure 4. Signal-to-control ratios resulting from different concentrations of HRP−TCP conjugate and 10 ng/mL TCP, where $n = 5$ for each point.

was under constant shaking, which is unfavorable for immuno binding. It was found that the incubation process needed 2 h to reach equilibrium for this static mode in a centrifuge tube. Also, such a long incubation time resulted in 10-fold stronger nonspecific binding than that from the fluidic immunoassay (data not shown).

The amount of HRP−TCP conjugate directly influenced the competition between the conjugate and the antigen and thus influenced the sensitivity of the competitive immunoassay of TCP. If the amount of HRP−TCP conjugate is very low, TCP and the conjugate cannot saturate the antibody coupled on the beads. Thus, all TCP in the sample and all conjugate will bind to the beads, which leads to a noncompetitive binding. When the amount of HRP−TCP conjugate is very high, the competition capability of TCP against HRP−TCP will be very weak. To determine the optimal amount of HRP−TCP used for the assay, CL signals with different concentrations of HRP−TCP conjugate were obtained from TCP at 10 ng/mL and PBS (as a control) in parallel. The signal-to-control ratio reached a minimum of 71% when the concentration of HRP−TCP conjugate was 2.0 μg/mL (Figure 4), indicating that the competition capability of TCP against HRP−TCP was the strongest under this condition. Therefore, HRP−TCP conjugate at 2.0 μg/mL was used in the competitive immunoassay.

Analytical Parameters of TCP Immunoassay. Under optimal conditions, the samples containing different concentrations of TCP were mixed with 2.0 μg/mL HRP−TCP conjugates and the mixed solution passed through the beads chamber with antibody-coupled beads trapped in it at a flow rate of 2.0 μL/min. After the substrate was delivered to the chamber, the resulting CL signal was recorded. It was found that the signals decreased with the increase of TCP concentration in the samples. The calibration curve for TCP showed a linear range of 0.20−70 ng/mL with a correlation coefficient of 0.990. The regression equation was $I = 72\,717 - 743.4C$ (ng/mL), where I is the CL intensity and C is the TCP concentration. A detection limit was estimated to be 0.080 ng/mL based on a signal/noise ratio of 3. The reproducibility of the TCP immunoassay using the microfabricated flow cell was assessed by intra- and interassay coefficients of variation (CV). The intra-assay CV was the difference between five determinations of one sample on the same flow cell. The interassay CV was the difference between the measurements of the same sample on five flow cells prepared in batch. Both intra- and inter- assay CVs were evaluated with TCP at low, medium, and high concentrations, and the results of a CV of 6.2−10.8% (Table 1) implied

Table 1. Intra- and Interassay Reproducibility for TCP Immunoassay

concentration (ng/mL)	intra-assay CV (%)	interassay CV (%)
1.0	8.1	9.1
10	10.8	6.4
50	6.2	7.5

Table 2. Analytical Recovery of TCP Spiked in Human Plasma Samples Obtained by the Designed Microfabricated Flow Cell

spiked concentration (ng/mL)	measured concentration (ng/mL)	analytical recovery (%)
1.0	0.81 ± 0.11	81
5.0	5.4 ± 0.40	108
10	11 ± 0.50	110
20	18 ± 1.0	90
50	43 ± 3.3	86

acceptable detection and fabrication reproducibility of this device. The entire fluidic assay process could be completed in 10 min in comparison to 2.5 h for static mode in a centrifuge tube.

Detection of TCP in Human Plasma. To evaluate its potential in clinical applications, this microfabricated beads-trapping/releasing flow cell was applied to human plasma samples spiked with standard TCP at five different concentrations. Table 2 displays the analytical recovery of different concentrations of TCP spiked in plasma obtained by the microfabricated device-based fluidic immunoassay. The analytical recovery of 81−110% for these spiked samples demonstrated its application potential in biological analysis for TCP.

CONCLUSIONS

An elastomer-microfabricated "beads injection" flow cell with trapping/releasing functions has been designed and fabricated for fluidic immunoassay. Compared to the reported disposable microfabricated devices, this device is reusable because a microstructured pillar-array filter combined with a pneumatic microvalve allows convenient trapping and releasing of beads. The microfabricated device is flexible for combining with various solid transducers and detectors. Using beads in the microchamber greatly improves the sensitivity and shortens the binding time, and therefore, it provides a fast and sensitive immunoassay tool. In this work, TCP has been measured as a model analyte in a competitive mode. Our further work is to apply it in a sandwich immunoassay of large-molecule analytes because we believe beads with a high surface-to-volume ratio can provide high sensitivity for a sandwich immunoassay. Besides being used for immunoassays, the microfabricated device can also be used for many other FI/SI solid-phase biochemical applications, such as ligand screening, DNA detection, and cell-based analysis.

ASSOCIATED CONTENT

Supporting Information. Additional information as noted in text. This material is available free of charge via the Internet at http://pubs.acs.org.

AUTHOR INFORMATION

Corresponding Author

*To whom correspondence should be addressed. E-mail: jun.wang@pnl.gov (J.W.); yuehe.lin@pnl.gov (Y.L.).

■ ACKNOWLEDGMENT

This work was supported partially by Grant U54 ES16015 from the National Institute of Environmental Health Sciences, the National Institute of Health (NIH), and Grant U01 NS058161-01 from the NIH CounterACT Program through the National Institute of Neurological Disorders and Stroke. Its contents are solely the responsibility of the authors and do not necessarily represent the official views of the federal government. A portion of the research was performed using the Microfabrication Laboratory in the Environmental Molecular Sciences Laboratory, a national scientific user facility sponsored by the U.S. Department of Energy's Office of Biological and Environmental Research and located at Pacific Northwest National Laboratory (PNNL). PNNL is operated for the U.S. Department of Energy by Battelle under Contract DE-AC05-76RL01830. Z.F. acknowledges a fellowship from PNNL and financial support from the Natural Science Foundation of China (20805036).

■ REFERENCES

(1) Zhao, L. X.; Sun, L.; Chu, X. G. *Trends Anal. Chem.* **2009**, *28*, 404–415.
(2) Ng, A. H. C.; Uddayasankar, U.; Wheeler, A. R. *Anal. Bioanal. Chem.* **2010**, *397*, 991–1007.
(3) Kloth, K.; Niessner, R.; Seidel, M. *Biosens. Bioelectron.* **2009**, *24*, 2106–2112.
(4) Mastichiadis, C.; Kakabakos, S. E.; Christofidis, I.; Koupparis, M. A.; Willetts, C.; Misiakos, K. *Anal. Chem.* **2002**, *74*, 6064–6072.
(5) Ho, J. A. A.; Wu, L. C.; Huang, M. R.; Lin, Y. J.; Baeumner, A. J.; Durst, R. A. *Anal. Chem.* **2007**, *79*, 246–250.
(6) Ozanich, R. M.; Bruckner-Lea, C. J.; Warner, M. G.; Miller, K.; Antolick, K. C.; Marks, J. D.; Lou, J. L.; Grate, J. W. *Anal. Chem.* **2009**, *81*, 5783–5793.
(7) Yang, Z. J.; Liu, H.; Zong, C.; Yan, F.; Ju, H. X. *Anal. Chem.* **2009**, *81*, 5484–5489.
(8) Wu, Y. F.; Zhuang, Y. F.; Liu, S. Q.; He, L. *Anal. Chim. Acta* **2008**, *630*, 186–193.
(9) Pollema, C. H.; Ruzicka, J. *Anal. Chem.* **1994**, *66*, 1825–1831.
(10) Soh, N.; Nishiyama, H.; Mishima, K.; Imato, T.; Masadome, T.; Asano, Y.; Kurokawa, Y.; Tabei, H.; Okutani, S. *Talanta* **2002**, *58*, 1123–1130.
(11) Tang, D. P.; Niessner, R.; Knopp, D. *Biosens. Bioelectron.* **2009**, *24*, 2125–2130.
(12) Marquette, C. A.; Coulet, P. R.; Blum, L. J. *Anal. Chim. Acta* **1999**, *398*, 173–182.
(13) Golden, J. P.; Floyd-Smith, T. M.; Mott, D. R.; Ligler, F. S. *Biosens. Bioelectron.* **2007**, *22*, 2763–2767.
(14) Bange, A.; Halsall, H. B.; Heineman, W. R. *Biosens. Bioelectron.* **2005**, *20*, 2488–2453.
(15) Whitesides, G. M. *Nature* **2006**, *442*, 368–373.
(16) Morozov, V. N.; Groves, S.; Turell, M. J.; Bailey, C. *J. Am. Chem. Soc.* **2007**, *129*, 12628–12629.
(17) Mulvaney, S. P.; Myers, K. M.; Sheehan, P. E.; Whitman, L. J. *Biosens. Bioelectron.* **2009**, *24*, 1109–1115.
(18) Hu, G. Q.; Gao, Y. L.; Li, D. Q. *Biosens. Bioelectron.* **2007**, *22*, 1403–1409.
(19) Yakovleva, J.; Davidsson, R.; Lobanova, A.; Bengtsson, M.; Eremin, S.; Laurell, T.; Emneus, J. *Anal. Chem.* **2002**, *74*, 2994–3004.
(20) Jonsson, C.; Aronsson, M.; Rundstrom, G.; Pettersson, C.; Mendel-Hartvig, I.; Bakker, J.; Martinsson, E.; Liedberg, B.; MacCraith, B.; Ohman, O.; Melin, J. *Lab Chip* **2008**, *8*, 1191–1197.
(21) Dong, Y.; Phillips, K. S.; Cheng, Q. *Lab Chip* **2006**, *6*, 675–681.
(22) Sung, W. C.; Chen, H. H.; Makamba, H.; Chen, S. H. *Anal. Chem.* **2009**, *81*, 7967–7973.
(23) Hofmann, O.; Voirin, G.; Niedermann, P.; Manz, A. *Anal. Chem.* **2002**, *74*, 5243–5250.
(24) Kong, J.; Jiang, L.; Su, X. O.; Qing, J. H.; Du, Y. G.; Lin, B. C. *Lab. Chip* **2009**, *9*, 1541–1547.
(25) Do, J.; Ahn, C. H. *Lab Chip* **2008**, *8*, 542–549.
(26) Bronzeau, S.; Pamme, N. *Anal. Chim. Acta* **2008**, *609*, 105–112.
(27) Sasso, L. A.; Undar, A.; Zahn, J. D. *Microfluid. Nanofluid.* **2010**, *9*, 253–265.
(28) Guan, X. A.; Zhang, H. J.; Bi, Y. N.; Zhang, L.; Hao, D. L. *Biomed. Microdevices* **2010**, *12*, 683–691.
(29) Sato, K.; Tokeshi, M.; Odake, T.; Kimura, H.; Ooi, T.; Nakao, M.; Kitamori, T. *Anal. Chem.* **2000**, *72*, 1144–1147.
(30) Lee, B. S.; Lee, J. N.; Park, J. M.; Lee, J. G.; Kim, S.; Cho, Y. K.; Ko, C. *Lab Chip* **2009**, *11*, 1548–1555.
(31) Endo, T.; Okuyama, A.; Matsubara, Y.; Nishi, K.; Kobayashi, M.; Yamamura, S.; Morita, Y.; Takamura, Y.; Mizukami, H.; Tamiya, E. *Anal. Chim. Acta* **2005**, *531*, 7–13.
(32) Shin, K. S.; Lee, S. W.; Han, K. C.; Kim, S. K; Yang, E. K.; Park, J. H.; Ju, B. K.; Kang, J. Y.; Kim, T. S. *Biosens. Bioelectron.* **2007**, *22*, 2261–2267.
(33) Unger, M. A.; Chou, H. P.; Thorsen, T.; Scherer, A.; Quake, S. R. *Science* **2000**, *288*, 113–116.
(34) Grover, W. H.; Skelley, A. M.; Liu, C. N.; Lagally, E. T.; Mathies, R. A. *Sens. Actuators, B* **2003**, *89*, 315–323.
(35) Liu, P.; Seo, T. S.; Beyor, N.; Shin, K. J.; Scherer, J. R.; Mathies, R. A. *Anal. Chem.* **2007**, *79*, 1881–1889.
(36) Skelley, A. M.; Scherer, J. R.; Aubrey, A. D.; Grover, W. H.; Ivester, R. H. C.; Ehrenfreund, P.; Grunthaner, F. J.; Bada, J. L.; Mathies, R. A. *Proc. Natl. Acad. Sci. U.S.A.* **2005**, *102*, 1041–1046.
(37) Hansen, C. L.; Classen, S.; Berger, J. M.; Quake, S. R. *J. Am. Chem. Soc.* **2006**, *128*, 3142–3143.
(38) Williamson, L. N.; Terry, A. V.; Bartlett, M. G. *Rapid Commun. Mass Spectrom.* **2006**, *20*, 2689–2695.
(39) Mauriz, E.; Calle, A.; Manclus, J. J.; Montoya, A.; Lechuga, L. M. *Anal. Bioanal. Chem.* **2007**, *387*, 2757–2765.
(40) Zou, Z. X.; Du, D.; Wang, J.; Smith, J. N.; Timchalk, C.; Li, Y. Q.; Lin, Y. H. *Anal. Chem.* **2010**, *82*, 5125–5133.